JOURNAL OF GEOPHYSICAL RESEARCH, VOL. 98, NO. B8, PAGES 13,851–13,862, AUGUST 10, 1993

Abyssal Hill Segmentation: Quantitative Analysis of the East Pacific Rise Flanks 7°S-9°S

JOHN A. GOFF[1]

Department of Geology and Geophysics, Woods Hole Oceanographic Institution, Woods Hole, Massachusetts

ALBERTO MALINVERNO, DANIEL J. FORNARI, AND JAMES R. COCHRAN

Lamont-Doherty Earth Observatory, Palisades, New York

The recent R/V *Maurice Ewing* EW9105 Hydrosweep survey of the East Pacific Rise (EPR) and adjacent flanks between 7°S and 9°S provides an excellent opportunity to explore the causal relationship between the ridge and the abyssal hills which form on its flanks. These data cover 100% of the flanking abyssal hills to 115 km on either side of the axis. We apply the methodology of Goff and Jordan (1988) for estimating statistical characteristics of abyssal hill morphology (rms height, characteristic lengths and widths, plan view aspect ratio, azimuthal orientation, and fractal dimension). Principal observations include the following: (1) the rms height of abyssal hill morphology is negatively correlated with the width of the 5- to 20-km-wide crestal high, consistent with the observations of Goff (1991) for northern EPR abyssal hill morphology; (2) the characteristic abyssal hill width displays no systematic variation with position relative to ridge segmentation within the EW9105 survey area, in contrast with observations of Goff (1991) for northern EPR abyssal hill morphology in which characteristic widths tend to be smallest at segment ends and largest toward the middle of segments; (3) abyssal hill rms heights and characteristic widths are very large just north of a counterclockwise rotating "nannoplate", suggesting that the overlap region is being pushed northward in response to microplate-style tectonics; and (4) within the 7°12'S-8°38'S segment, abyssal hill lineaments are generally parallel to the ridge axis, while south of this area, abyssal hill lineaments rotate with a larger "radius of curvature" than does the EPR axis approaching the EPR-Wilkes ridge-transform intersection.

INTRODUCTION

Abyssal hill morphology forms through a complex combination of tectonic (surface faulting) and constructional (volcanic) processes which occur at or near the ridge axis. The morphology of these structures is then modified through time by sedimentation, mass wasting, and volcanic overprinting. Inasmuch as the processes and the morphology are related, the texture of the seafloor represents a time and space series record, albeit an indirect one, of the ridge crest system. The recent R/V *Maurice Ewing* EW9105 survey of the East Pacific Rise (EPR) and adjacent flanks 7°S-9°S [*Cochran et al.*, 1993] (Plate 1) provides an excellent opportunity to explore the causal relationship between the accreting process at the ridge axis and abyssal hills which form on its flanks. The Hydrosweep multibeam bathymetric data [*Chayes et al.*, 1991] provided 100% coverage of the flanking abyssal hills to 115 km on either side of the axis. Along-axis this section of the ridge includes a complete 165-km-long segment bounded by a second-order discontinuity to the north and a third-order discontinuity to the south (see *Macdonald et al.* [1988] for full explanation of discontinuity terminology).

In past work, a methodology has been established for estimating statistical characteristics of abyssal hill morphology (rms height, characteristic lengths and widths, plan view aspect ratio, azimuthal orientation, and fractal dimension) and available multibeam bathymetric data has been analyzed [*Goff and Jordan*, 1988; 1989*a*, *b*; *Goff*, 1991; 1992]. Two principal conclusions were drawn from these works. Greatly simplified, they are that (1) a significant amount of variation in abyssal hill characteristics can be correlated with spreading rate, while (2) after accounting for spreading rate dependence, a significant amount of variation remains; i.e., more factors than just spreading rate affect the formation of abyssal hills.

One possible explanation for variation in seafloor characteristics unattributable to spreading rate variation was discovered along the EPR 9°-15°N, where a high density of multibeam data exists [*Goff*, 1991]. The rms height and characteristic widths estimated from this region exhibit a negative and positive correlation respectively with the depth of the rise axis and, by inference, with the relative abundance in magma supply feeding the ridge. The hypothesis that magma supply exerts a strong influence on the formation of abyssal hills is important both for the interpretation of abyssal hill texture off-axis and for constraining models of ridge faulting and magmatism at fast spreading mid-ocean ridges.

Hydrosweep data coverage from the EW9105 cruise allow us to go a step further in the quantitative analysis of near-ridge abyssal hills. The Hydrosweep multibeam system allows for 90° swath coverage, or approximately twice the water depth. Track spacing for the EW9105 survey was dense enough to obtain complete coverage with track lines oriented perpendicular to the ridge, and the survey area extends far enough from the ridge to allow four corridors of analysis (Figure 1): two corridors just east and west of the ridge out to ~50 km from the rise axis (corridors E1 and W1) and two more between ~50 km from the rise axis and the farthest extent of the survey (corridors E2 and W2). These corridors will allow us to analyze axial asymmetry in the formation of abyssal hills

[1] Now at University of Texas Institute for Geophysics, Austin.

Paper number 93JB01095.
0148-0227/93/93JB-01095$05.00

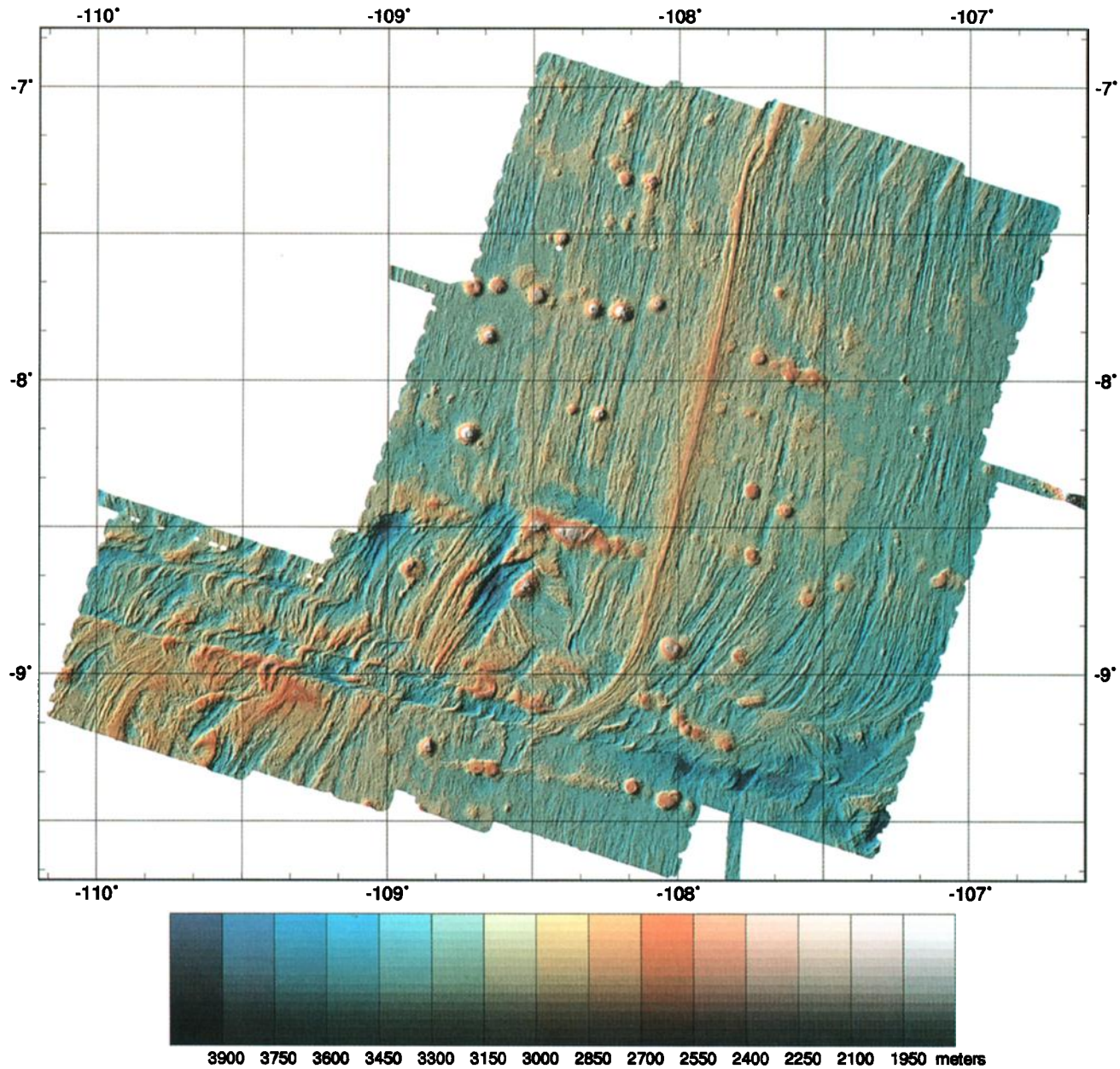

Plate 1. Color-contoured gray-shaded relief plot of the Hydrosweep bathymetry from the EW9105 cruise. Illumination angle is from the west.

and allow a rudimentary investigation of temporal variations over the past 1 m.y.

There is currently a stark lack of knowledge concerning how the process of abyssal hill formation is governed by ridge-axis variables. Thus any attempt to characterize the ridge environment from abyssal hill data will be highly speculative. The primary purpose of this work is to continue to document the quantitative relationship between abyssal hills and the characteristics of the ridge crest system which created them. We expect this work to help form a basis for interpretation of off-axis morphology in terms of ridge-crest variables and to impose constraints which must be satisfied by any successful model of abyssal hill formation.

FORMATION OF ABYSSAL HILLS AT FAST SPREADING RATES

Several studies have attempted to track to one degree or another the formation of surface morphology from the moment of rifting to the cessation of tectonic and volcanic activity along the flanks of the EPR. These include studies along the Rivera [*Lewis*, 1979; *CYAMEX*, 1981; *Macdonald and Luyendyk*, 1985], Cocos [*Choukroune et al.*, 1984], and Nazca [*Lonsdale*, 1977; *Searle*, 1984; *Renard et al.*, 1985; *Bicknell et al.*, 1987] spreading sections of the East Pacific Rise.

A series of generic stages for the formation of abyssal hills was developed by *CYAMEX* [1981] and modified by *Macdonald and Luyendyk* [1985] (see also *Goff* [1991, Figure 4]) on the basis of submersible observations along the Rivera spreading section of the East Pacific Rise. Proceeding outward from the axis, these include (1) ridge axis volcanism, including flood basalt and edifice formation, (2) fissuring and horst and graben formation, with no polarization in faulting direction, (3) polarized normal faulting with larger inward facing faults driven by necking of the lithosphere [*Tapponnier and Francheteau*, 1978; *Phipps-Morgan et al.*, 1987; *Lin and Parmentier*, 1989; *Chen and Morgan*, 1990], leading to the

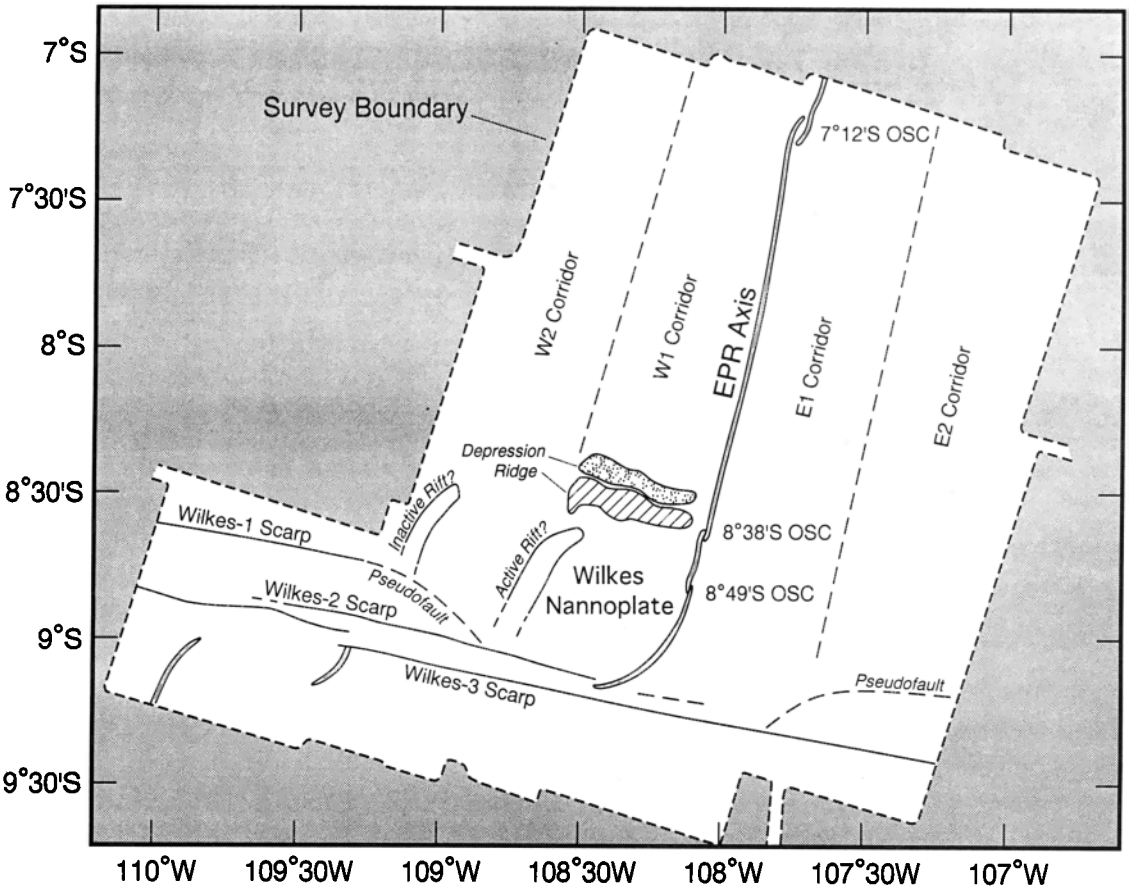

Fig. 1. Schematic drawing of the primary morphological structures which can be seen in the EW9105 survey area (compare with Plate 1). Also shown are the approximate boundaries of the four corridors (W1, W2, E1, and E2) which serve as the regionalization for quantitative analysis.

formation of a rift valley, and (4) cessation of abyssal hill construction, with morphology slowly modified by mass wasting, sedimentation, and occasional off-axis volcanism.

Fast spreading ridges (>~80 mm/yr full rate) apparently undergo only the first two of the abyssal hill construction stages. Rather than a rift valley, the plate boundary is marked by a ridge crest which is likely to be an isostatic response to a buoyant zone of partial melt in the upper mantle beneath the rift [*Madsen et al.*, 1984]. The large volume and inferred high eruption rates of basalts flows from the rift create an exterior morphology akin to a linear shield volcano [*Lonsdale*, 1977]. The locus of volcanic activity is generally continuous within a spreading section [*Lonsdale*, 1977], implying that the magma supply is predominantly steady state, though subject to temporal and spatial variations in intensity [*Macdonald and Fox*, 1988].

The lid of the magma chamber or lens beneath fast spreading ridges is approximately 1-2 km deep and 1-2 km wide [*Sinton and Detrick*, 1992]. The presence of a thin brittle layer atop the magma chamber prevents the development of large relief in the beginning stages of fissuring and horst and graben formation [*Lonsdale*, 1977]. Large-scale horst and graben formation, leading to full scale abyssal hills, is observed to begin, often abruptly, 2-10 km from the ridge crest [*Lonsdale*, 1977; *Choukroune et al.*, 1984, *Bicknell et al.*, 1987; *Edwards et al.*, 1991]. *Lonsdale* [1977] attributed this onset to the laterally transported material reaching the edge of the subaxial magma chamber. *Lister* [1977] postulated that with the transition between magma chamber and deep brittle crust comes a sudden onslaught of hydrothermal penetration, perhaps sufficiently cooling the upper crust to initiate large extensional structures. It is unlikely, however, on the basis of seismic data that the axial magma chamber extends this far from the rise axis [*Detrick et al.*, 1987; *Sinton and Detrick*, 1992]. *Goff* [1991] suggested that the onset of large-scale abyssal hill faulting may be coincident with the edge of the partial melt/low-viscosity zone. Such a zone has been postulated to satisfy both gravimetric [*Madsen et al.*, 1984] and seismic [*Burnett et al.*, 1989; *Toomey et al.*, 1990] constraints. *Chen and Morgan* [1990], in modeling rift dynamics, postulated that such a zone would mechanically decouple the viscous flow from the plate. On the basis of this work *Edwards et al.* [1991] suggest that such decoupling could reduce the influence of the regional stress regime on the overlying crust. Thus the onset of full-scale faulting in fast spreading regions may mark the location of full mechanical coupling between upper and lower lithosphere. Alternatively, *Goff* [1991] postulated that the partial melt zone may act as a thermal buffer. In this scenario, rapid cooling, and by consequence the buildup of thermal stress and attendant surface tectonism, would not begin in earnest until after the crust passed the off-axis extent of the partial melt zone.

The question of whether abyssal hills are formed primarily by volcanism or tectonism has been addressed in previous work. *Lonsdale* [1977] interpreted the topography along a deep-tow profile taken across the East Pacific Rise at 3°25'S as almost entirely faulted in origin. *Bicknell et al.* [1987], interpreting deep-tow profiles at 19°30'S, concluded that the intermediate wavelength (2-8

km) topography off axis has a faulted origin, while the short-wavelength topography (a few hundred meters) has a volcanic origin.

EAST PACIFIC RISE BETWEEN 7°S AND 9°S

Details regarding the East Pacific Rise and Wilkes transform in the vicinity of the survey area are given by *Cochran et al.* [1993] and *Goff et al.* [1993]. Relevant points are summarized here.

The surveyed section of the EPR north of the Wilkes transform includes one second-order discontinuity [*Macdonald et al.*, 1988], an 8-km overlapping spreading center (OSC) at 7°12'S, and two third-order discontinuities, a <1 km offset OSC at 8°49'S and a ~1.2 km offset OSC at 8°38'S (Figure 1). Although the offset is very small at the 8°38' OSC, this discontinuity serves as a significant morphological boundary. The minimum axial depth changes by more than 50 m across it, with 40 m of the change occurring in less than 1 km at the southern tip of the northern ridge segment. In addition, a large 10-km-wide east-west trending ridge standing over 1 km above the surrounding seafloor extends away from this OSC to the west.

The origin of this east-west trending ridge is of particular interest. To the south of the this ridge and west of the rise axis is a zone of highly disrupted morphology bounded ~50 km off axis by a rift with over 1 km of vertical relief. On the basis of high acoustic backscatter within this rift it is inferred to be currently active [*Goff et al.*, 1993]. *Goff et al.* [1993] have identified the region between the EPR axis and this secondary rift as a distinct lithospheric block, identified as the Wilkes "nannoplate", that it is currently rotating counterclockwise in accordance with the *Schouten et al.* [1993] hypothesis for edge-driven microplate kinematics. *Goff et al.* [1993] identify the east-west trending ridge emanating from the 8°38'S OSC wholly or in part as a compressional feature. This interpretation is supported both by observations of an apparent downwarping just north of the ridge (Figure 1) and by observations that the positive free-air gravity anomaly across this feature is larger by a factor of almost 2 than the anomalies observed over nearby seamounts of similar size [*Goff et al.*, 1993].

In contrast with the undulating axial depth variations exhibited by the northern EPR axis [*Macdonald and Fox*, 1988], the surveyed portion of the southern EPR axis has a nearly constant depth of about 2725 m for a distance of about 140 km from 7°22'S to 8°35'S (Figure 2). Although the shallowest axial depth (2699 m) is located near the center of the segment at 7°45.4'S, 20-30 m variations in axial depth along the segment do not systematically decrease as the segment ends are approached. Furthermore, the axial zone, viewed as the inner few kilometers of the crestal high [*Macdonald and Fox*, 1988] has a very uniform flat-topped appearance between the OSCs at 7°12'S and 8°38'S. These observations led *Cochran et al.* [1993] to hypothesize that, along the superfast spreading southern EPR, there is a broad, well-connected area of elevated temperatures beneath the axis, so that a relatively efficient subcrustal shallow magmatic plumbing system extends the length of the ridge segment. This is in contrast to the situation hypothesized for the northern EPR, which apparently has a less efficient plumbing system and cannot deliver magma evenly along the length of the ridge segment.

Despite the constancy of the axial depth and shape of the axial zone, the width of the crestal high, considered as the entire 5- to 20-km-wide bathymetric high, varies considerably along-strike between the 7°12'S and 8°38'S OSCs (Figures 2 and 3). This feature, interpreted as a flexural-isostatic response to the low-density region under the ridge axis and thus indicative of the pattern of deep upwelling [*Madsen et al.*, 1984, 1990; *Wang and Cochran*, 1993], is widest in the middle of the segment and tapers off toward the ends. This is similar to the crestal high morphology observed along segments bounded by second order discontinuities on the northern EPR. *Cochran et al.* [1993] hypothesize that deep upwelling beneath southern EPR segments is focused in some region within the segment.

Cochran et al. [1993] thus identify a "deep" and a "shallow" magma supply. The "deep" magma supply is the melt production caused by the focused upwelling of hot mantle material beneath the spreading axis and has a similar structure for both northern and southern EPR segments. The "shallow" magma supply consists of the plumbing system which delivers melt to the surface and is much more efficient for southern EPR segments than northern EPR segments.

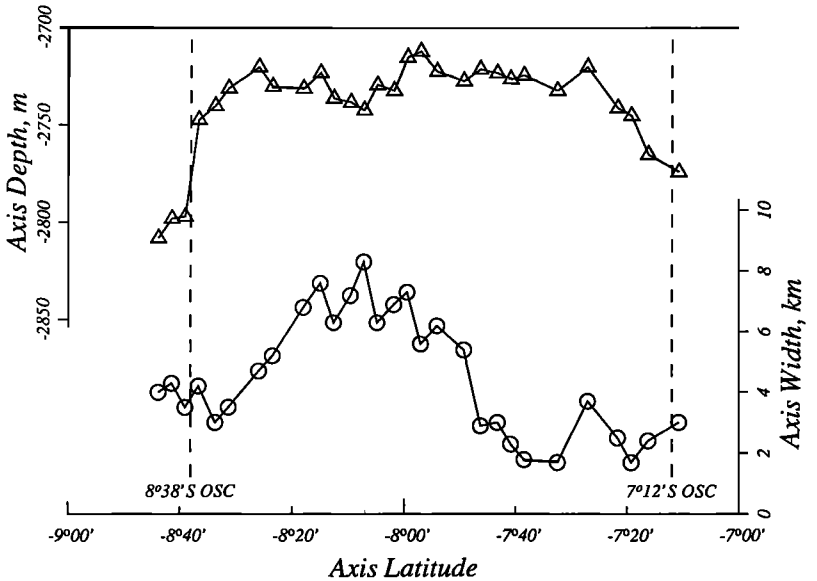

Fig. 2. Minimum axial depth (top, triangles) and axial width (bottom, circles) plotted as functions of axis latitude (the location where the track line of the Hydrosweep data used for measurement crosses the axis). Axial width is determined by the distance between points 200 m deeper than the axis to either side. Adapted from *Cochran et al.* [1993].

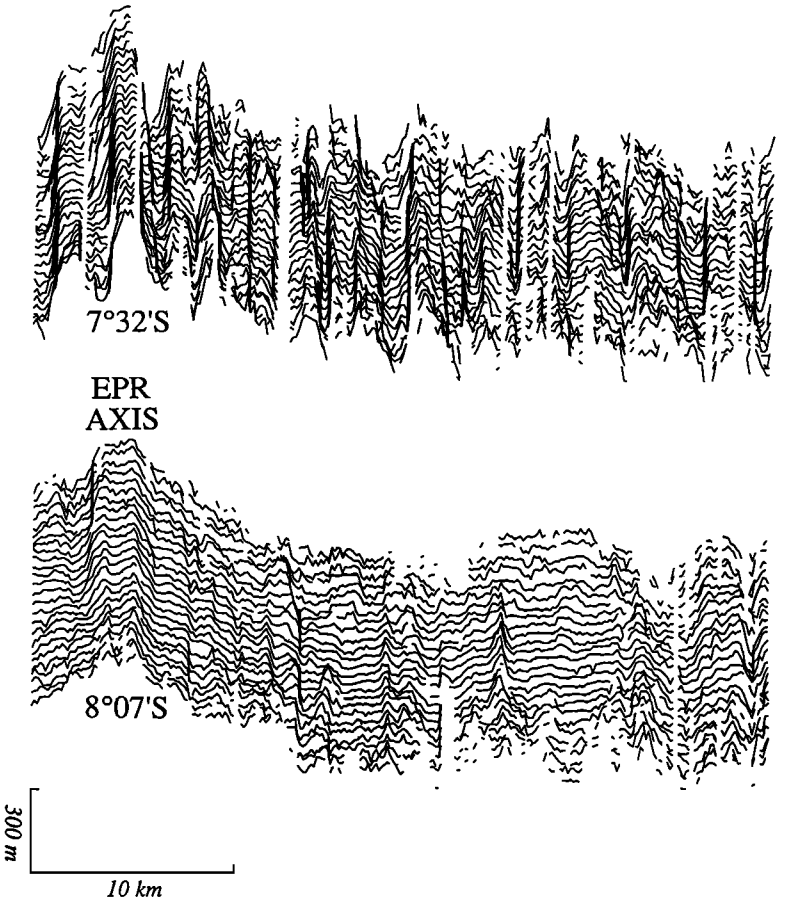

Fig. 3. Two Hydrosweep swaths which cross the EPR axis and a portion of the eastern flank. Figures were created by plotting individual Hydrosweep beam profiles side by side. This gives an exaggerated three-dimensional perspective. The width of each swath is approximately 6 km. The swath crossing the axis at 7°32'N, toward the northern end of the segment, exhibits a thinner axial high and larger abyssal hills than the swath crossing the axis at 8°07'S, closer to the middle of the segment.

STOCHASTIC CHARACTERIZATION

The stochastic model used to characterize the second-order statistics of abyssal hill morphology and the procedure for inverting model parameters from Sea Beam data are given in detail by *Goff and Jordan* [1988, 1989*a*, *b*] and summarized by *Goff* [1991, 1992]. The methodology of stochastic characterization takes as input a swath of multibeam data and produces as output estimates of relevant physical parameters with formal uncertainties. Two criteria are placed on swaths chosen for input: (1) they are along relatively straight track lines and long enough to produce well-resolved estimations [*Goff and Jordan*, 1989*b*], and (2) the morphology sampled does not include seamounts or the axial bulge (to the best of our ability to identify these features).

The output physical parameters include the following:

1. The rms height is the average variation of bathymetry about the mean depth.

2. The orientation of topography is the azimuth of the strike of abyssal hill lineaments.

3. The characteristic length is the visually dominant feature length (or wavelength) along a profile direction. It is defined by the width of the covariance along the same profile direction [*Goff and Jordan*, 1988]. Perpendicular to the grain it is called the characteristic width of abyssal hills and parallel to the grain it is called the characteristic length.

4. The aspect ratio is the characteristic planar shape of the abyssal hills.

5. The Hausdorff (fractal) dimension is a measure of roughness. It is defined by the asymptotic properties of the covariance function as the lag $\rightarrow$ 0. An increase in fractal dimension represents an increase in roughness, the limiting cases of 2 and 3 corresponding to a random field with continuous derivative (Euclidean surface) and one which is space filling (Peano surface), respectively.

These parameters and their uncertainties form an objective basis for morphological classification; i.e., for stating that one region is significantly different from another region and what makes them different. What these parameters cannot do at present is tell us, for example, that a certain region is dominated either by extensional tectonism or constructional volcanism. These processes are dissimilar, and it is not unreasonable to expect that the morphologies they produce will have characteristic differences which can be detected with the estimated stochastic model parameters. Unfortunately, at the scales considered here, we do not yet have the ability to make this distinction. We are thus unable, with our current methodology, to test either hypotheses regarding the characteristics of volcanic versus tectonic terrain or hypotheses regarding the relative contribution of each in different regions. However, in combination with what we know about ridge crest processes and their segmentation, the results presented here can be

used as the basis of formulating reasonable hypotheses for later testing.

RESULTS

We have elected to focus on the three most robustly resolved parameters: the rms height, characteristic width, and lineament azimuth of abyssal hill morphology. For the short characteristic widths which generally exist along the EPR, the fractal dimension is very difficult to estimate with satisfactory accuracy [*Goff and Jordan*, 1989*b*]. Similar to estimation of higher-order parameters [*Goff*, 1991], estimation of the fractal dimension is not a sensitive means of terrain classification on a regional scale. Uncertainties on the estimation of characteristic length and plan view aspect ratio are also quite large compared to its observed variation within the EW9105 data set.

The common format chosen to present the data is to plot estimated parameters versus axis latitude (the location where the track line extending from the Hydrosweep data used for inversion crosses the axis). Estimated parameters for each corridor (Figure 1) are plotted using a common symbol. As a compromise between visibility and comparability, the west corridor results are placed on a separate plot from the east corridor results. Owing to volcanic overprinting (i.e., seamounts) throughout, the western corridors are not as well-sampled as the eastern corridors. Parameters were not estimated along the western corridors south of the ridge emanating from the 8°38' OSC which delimits the northern boundary of the Wilkes nannoplate (Plate 1 and Figure 1). The locations of the 8°38'S and 7°12'S OSCs are identified on each plot.

RMS Abyssal Hill Height

Estimated rms abyssal hill heights for all four corridors are plotted in Figure 4. The principal observation is clear: within the ridge segment bounded by the 8°38'S and 7°12'S OSCs, and across all four corridors, the rms height is least toward the middle of the segment and increases toward the ends of the segment. This, the most robust observation to be presented in this paper, is consistent with the observations of *Goff* [1991] along the flanks of the EPR between 8°N and 16°N.

The correlation between abyssal hill rms height and the width of the crestal high is evident in comparison of Figures 2 and 4, and is shown in Figure 3. The two swaths plotted in Figure 3 are from a crossing near the northern end of the segment (top panel) and from near the center of the segment (bottom panel). The northern swath exhibits a narrower crestal high and larger rms abyssal hill variation than does the central swath.

Comparison between corridors (Figure 4) reveals the following deviations from uniformity. First, while the minimum rms height (~40-45 m) is approximately at axis latitude 8° for the W1 and E1 corridors, the minimum rms height along the E2 corridor (~35-40 m) is spread among three swaths ranging from axis latitudes 7°36'S to 7°51'S. The W2 corridor appears to have a similar northward shift in rms height minimum, though the W2 corridor is not sampled well enough to make this observation robust. Second, rms heights on the W1 corridor increase dramatically faster approaching the 8°38'S OSC than either the E1 or E2 corridor, resulting in a 40-50 m disparity across axis. The W2 corridor also exhibits a large increase in rms height approaching the 8°38'S OSC but not as large a change as along the W1 corridor and not sufficiently large to confidently distinguish from rms heights estimated within the adjacent eastern corridors. Possible hypotheses which account for these observations will be presented in the Discussion section.

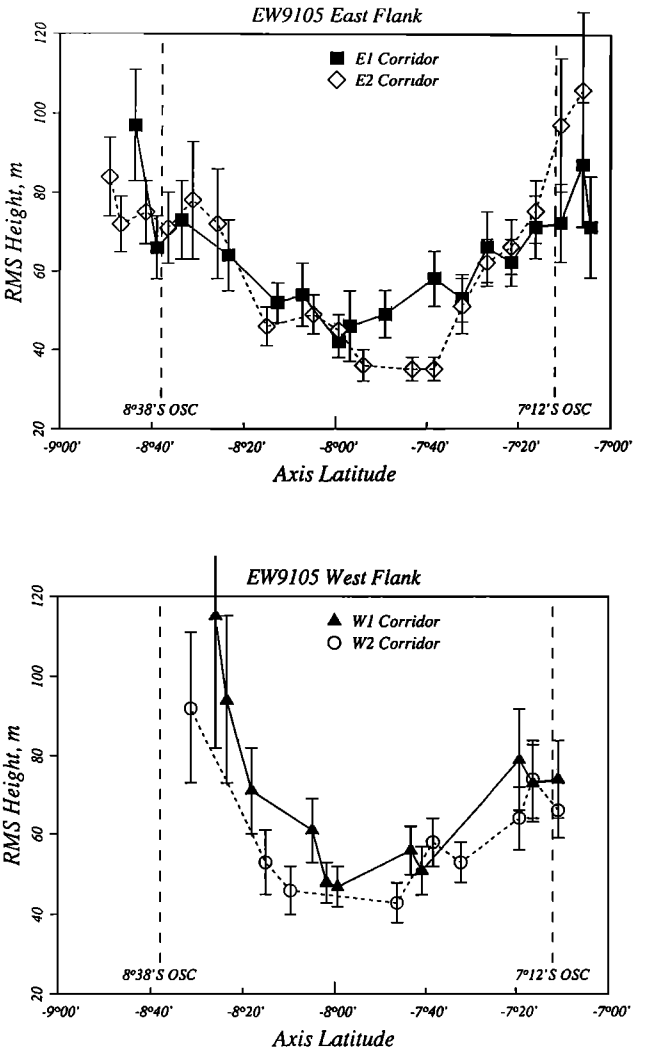

Fig. 4. Estimated rms heights plotted as a function of axis latitude (the location where the track line extending from the Hydrosweep data used for inversion crosses the axis) for each of the four corridors. Vertical bars represent 1 σ error estimates.

Characteristic Abyssal Hill Width

Estimated characteristic abyssal hill widths for all four corridors are plotted in Figure 5. With the exception of estimates near the 8°38'S OSC and a single estimate near 7°54'S on the E1 corridor, there is no recognizable systematic variation in characteristic width along the segment between the 8°38'S and 7°12'S OSCs. Throughout this region, estimates appear randomly scattered between values of ~1.8-5 km. This behavior is in contrast to northern EPR segments, where abyssal hill characteristic widths are generally found to be largest toward segment centers (or where the crestal high is widest) and smallest toward the segment ends (or where the crestal high is thinnest), also resulting in a negative correlation between rms height and characteristic width [*Goff*, 1991].

The primary exception to a lack of systematic variation in characteristic width occurs near the 8°38' OSC. Here the W1 and W2 corridors exhibit large increases in very similar fashion and proportion as their respective increases in rms height (Figure 4). The errors on these estimates are large because the characteristic width is a significant fraction of the swath length [*Goff and Jordan*, 1989*b*]. However, in this case, visual examination is sufficient to

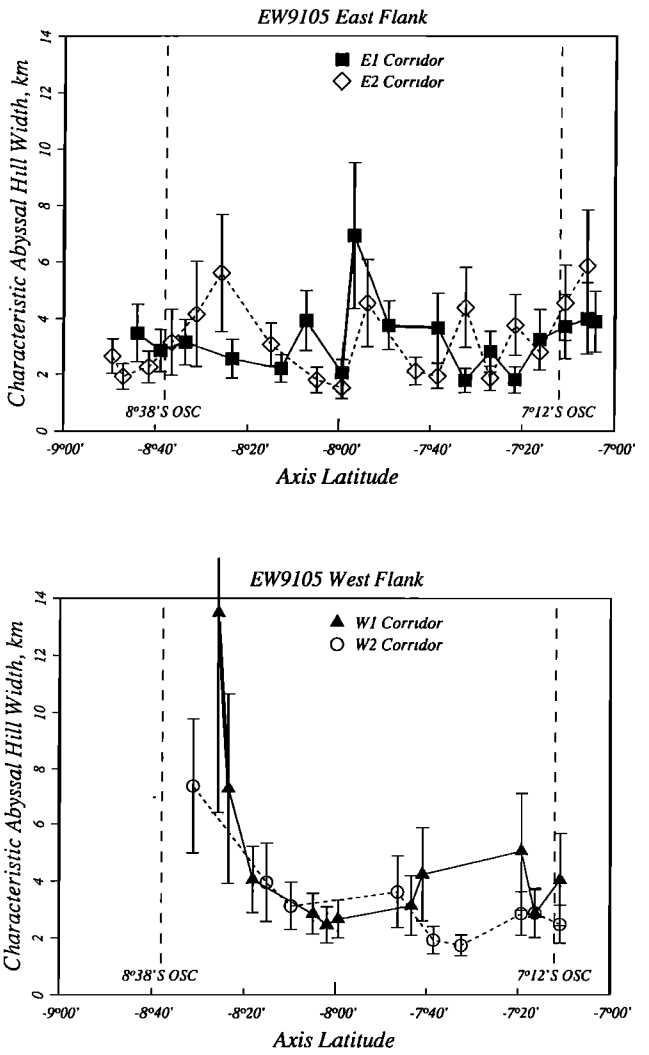

Fig. 5. Estimated characteristic abyssal hill widths plotted as a function of axis latitude (the location where the track line extending from the Hydrosweep data used for inversion crosses the axis) for each of the four corridors. Vertical bars represent 1σ error estimates.

confirm that approaching the ridge adjacent to the 8°38'S OSC along the W1 corridor, there is a dramatic increase in the size and characteristic width of abyssal hill morphology. This point is demonstrated in Figure 6.

Characteristic widths along the E2 corridor also increase in the vicinity of the 8°38'S OSC, though not by as much as the western corridors. South of 8°38'S, E2 characteristic widths decrease markedly, despite the fact that rms heights in this region are generally constant (Figure 4). Characteristic widths along the E1 corridor are not resolvably different throughout the southern region portion of the survey area.

Abyssal Hill Lineament Azimuth

Estimated abyssal hill lineament azimuths for all four corridors are presented in Figure 7 along with the ridge axis azimuth. Within most of the 8°38'S-7°12'S segment, and aside from the erratic behavior of two samples near the middle of the segment along the E1 corridor, abyssal hill lineaments in this region are roughly parallel to the ridge crest at the same axis latitude. Lineament azimuths along well-sampled east flank corridors rotate from ~N015°E at 8°20'S to ~N008°E at ~7°30'S and back to ~N015°E at just south of the 7°12'S OSC. This subtle "S"-shaped curvature is nearly identical to the variation in ridge-axis azimuth at these axis latitudes. This pattern is not as clearly present in the more poorly sampled west flank corridors.

North of the 7°12'S OSC, the ridge axis trends at ~N020°E. Within the OSC, axis trends exceed N030°E. Abyssal hill lineaments also rotate clockwise going northward across this OSC, with a variety trends ranging from ~N018°E to ~N030°E at the northernmost swaths. As with variations in the rms height in this vicinity (Figure 4), this variation may reflect interaction with the off-axis trace of the large 7°12'S OSC.

Abyssal hill lineaments along the E1 and E2 corridors systematically rotate from ~N015°E at 8°14'S along the E1 corridor and at 8°25'S along the E2 corridor to ~N036°E close to the Wilkes transform complex. This behavior approximately mimics the curvature of the ridge axis as it enters the ridge-transform intersection. However, the abyssal hill lineament rotation has a larger "radius of curvature" than and is shifted 25-40 km north of the axis curvature. Furthermore, abyssal hill curvature along the E1 corridor begins ~20 km north of where abyssal hill curvature begins along the E2 corridor.

DISCUSSION

Abyssal Hill Segmentation

From data presented both within this paper for the southern EPR and by *Goff* [1991] for the northern EPR, it is evident for fast and very fast spreading ridges that the rms height of flanking abyssal hills is least toward the middle of ridge segments and largest at the ends. *Goff* [1991] inferred from this observation a negative correlation between rms height and the magma supply, the factor which *Macdonald and Fox* [1988] identified as the principal variable in ridge segmentation. However, assuming that the process of abyssal hill formation is similar at fast and very fast spreading rates, the observations of *Cochran et al.* [1993] regarding the variation of axial depth and shape along the 8°38'S-7°12'S segment force us to refine this conclusion. If as hypothesized the nearly level axial depth (Figure 2) and uniform appearance of the axial zone imply evenly distributed magma supply along axis within a melt lens, then it is unlikely that this "shallow" magma supply is a primary a factor affecting the systematic variation in abyssal hill rms height. On the other hand, the width of the 5-20 km crestal high does change systematically, both along northern and southern EPR segments, in a manner that correlates well with rms height variations (compare Figures 2 and 3). We therefore infer that the variation in abyssal hill rms heights is correlated with the upwelling/temperature structure beneath the ridge and/or with the size of the partial melt zone (the "deep" magma supply).

The distinction between a correlation with "deep" versus "shallow" magma supply should be an important constraint in the modeling of abyssal hill formation. If the "shallow" magma supply (the supply of magma in the upper mantle or crustal reservoir that directly feeds axial volcanism) is nearly constant along axis, then the variation in abyssal hill rms height with segmentation is unlikely to be caused by variations in volcanic construction. Rather, the size of surface normal faults must be the primary variable.

Why, then, would surface faulting be influenced by the upwelling/temperature structure and/or the size of the partial melt zone beneath the axis? Two suggested mechanisms for faulting include amagmatic extension [e.g., *Bicknell et al.*, 1987] and

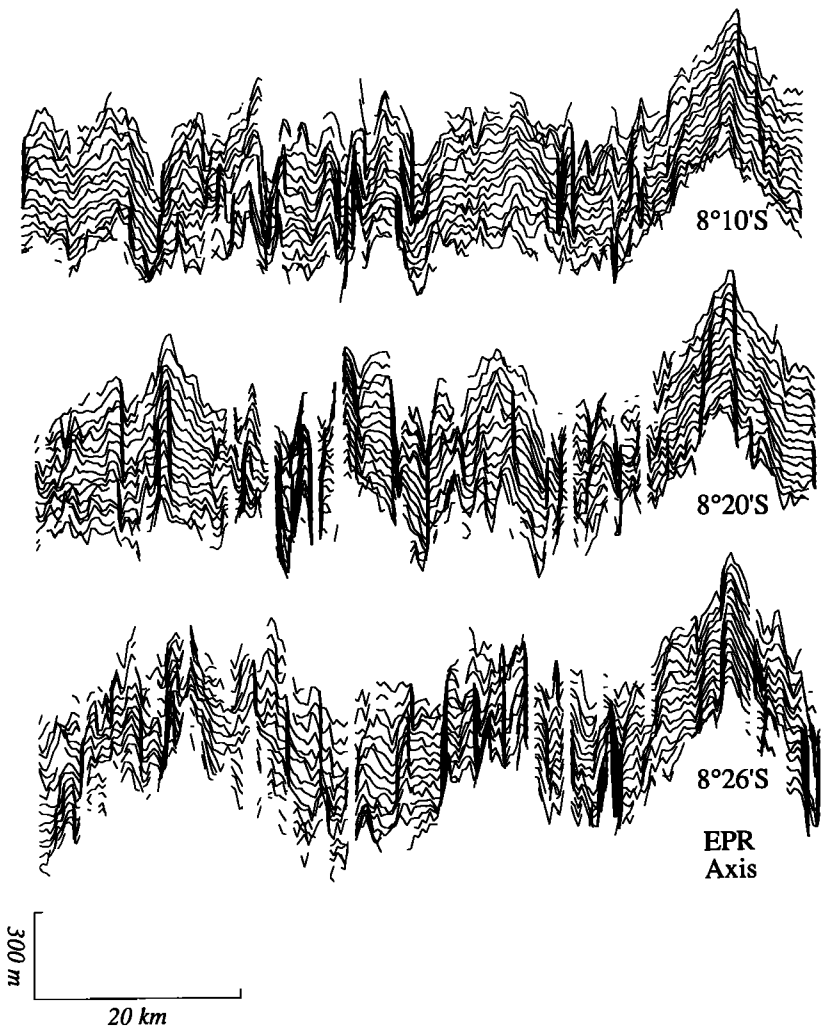

Fig. 6. Three successive Hydrosweep swaths along the W1 corridor approaching the transverse ridge adjacent to the 8°38'S OSC (see Plate 1 and Figure 1). Figures were created by plotting individual Hydrosweep beam profiles side by side. This gives an exaggerated 3-D perspective. The width of each swath is approximately 6 km. Top panel crosses the EPR axis at 8°10'S, the middle panel at 8°20'S, and the bottom panel at 8°26'S. These data visually demonstrate a large increase both in the rms height and characteristic width of abyssal hills approaching the 8°38'S transverse ridge.

thermal contraction [*Goff*, 1991]. There are several possible ways that variations in the thermal structure and/or the size of the partial melt zone may affect faulting by either mechanism [*Goff*, 1991]. First, the temperature structure will affect the thickness of the brittle layer. A wider partial melt zone toward the middle of segments implies higher lithospheric temperatures adjacent to the axis (where abyssal hills are formed). We thus expect a thicker brittle layer toward the ends of the segments and consequently the ability to support larger faults. However, ability to support larger faults does not explain why larger faults exist. Larger faults require greater stresses to form [e.g., *Forsyth*, 1992], so we must explain the existence of greater stress. Furthermore, since the characteristic width does not correlate with rms height, it is likely that the total strain is roughly proportional to the fault offset or height (provided that fault dip remains approximately constant). Hence it is probable that the brittle lithosphere undergoes greater tectonic extension adjacent to ridge segment ends than adjacent to the middle of segments.

The mechanical and/or thermal properties of a partial melt zone may help explain why there might be greater stress and/or greater amount of extension at ridge segment ends. *Goff* [1991] considered two possibilities. (1) The partial melt zone may act as a mechanical buffer, decoupling crustal deformation from deeper regional stresses [e.g., *Chen and Morgan*, 1990; *Edwards et al.*, 1991]. If true, then the onset of full-scale faulting in fast spreading regions may mark the location of full mechanical coupling between upper and lower lithosphere. A wider partial melt zone would thus maintain the decoupling for a longer time, with the end result of surface tectonism reflecting a smaller amount of the total lithospheric extension. This scenario could be important for either amagmatic extension or thermal contraction. (2) The partial melt zone may act as a thermal buffer. In this scenario, applicable only to the thermal contraction model, rapid cooling, and by consequence the build up of thermal stress and attendant surface tectonism, would not begin in earnest until after the crust passed the off-axis extent of the partial melt zone. Thermal buffering could allow cooling to occur slowly for a time, so that when rapid cooling begins, there is a smaller temperature drop, and thus less thermal stress and less total extension reflected at the surface.

"Smooth" Spot

The minimum rms heights along the E2 corridor are smaller than and shifted northward of the minimum rms heights for the E1 corridor (Figure 4). This "smooth" spot is easily noticeable in the eastern end of the survey area (Plate 1) centered about 8°S. To the

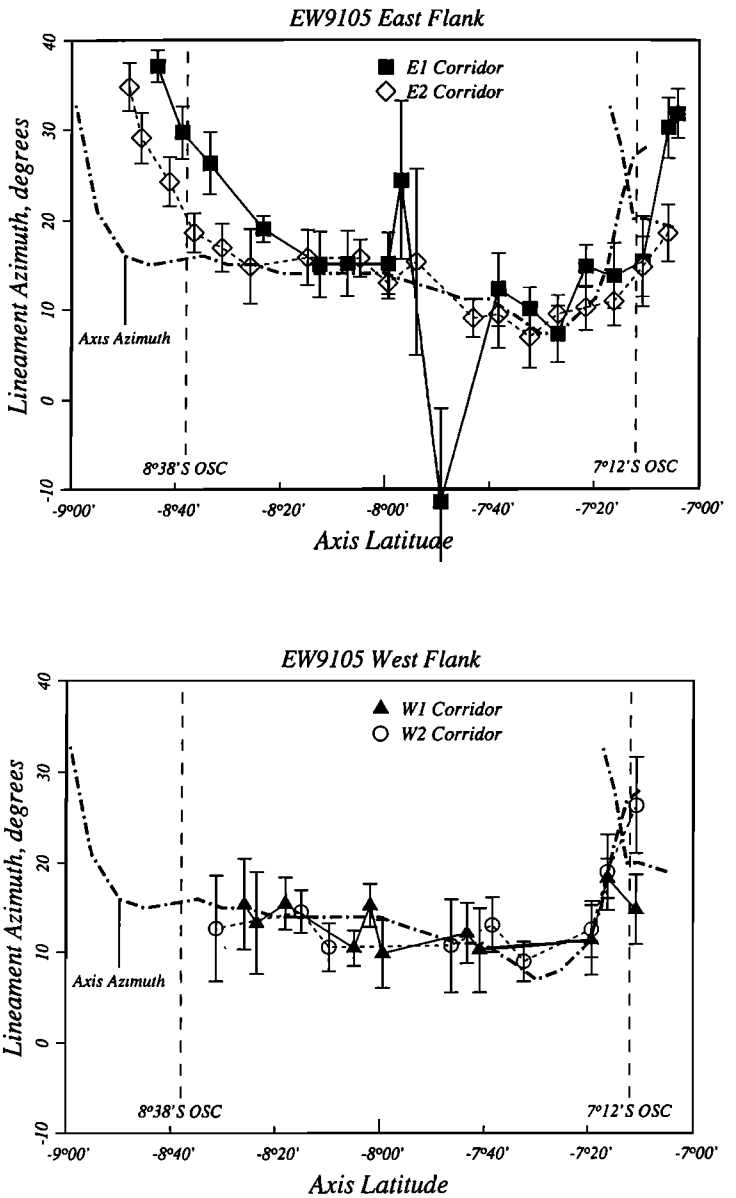

Fig. 7. Estimated lineament azimuths plotted as a function of axis latitude (the location where the track line extending from the Hydrosweep data used for inversion crosses the axis) for each of the four corridors. Vertical bars represent 1σ error estimates. Heavy dashed line represents the axis azimuth.

extent that abyssal hill rms heights are correlated with the upwelling/temperature structure of the ridge, this shift in minima latitude may reflect temporal variation in the focusing of mantle upwelling. However, given that we cannot, due to poorer sampling, conclusively make the same observation on the western flank, we cannot discount the possibility that the E2 corridor has been overprinted with off-axis sheet flows. A few small seamounts do exist in the area (Plate 1). While seamounts and like features are easily removed from the data prior to analysis, there is no way to identify, and thus avoid, sheet flows.

Characteristic Width

Characteristic widths appear to be correlated with segmentation adjacent to the northern EPR [*Goff*, 1991], whereas in the EW9105 survey there is no apparent correlation. It is thus possible that this parameter could be partly controlled by the "shallow" magma supply, which likewise varies systematically along the individual segments on the northern EPR while being nearly constant along individual segments on the southern EPR [*Cochran et al.* 1993]. This leads us to speculate that volcanism may be a significant contributing factor to the formation of abyssal hills at fast spreading rates.

Although it is apparent that volcanic constructs of the type produced at slow spreading rates [*CYAMEX*, 1981, and references therein; *Kong et al.*, 1988; *Smith and Cann*, 1990] do not exist at these fast spreading rates, we envision the possibility of large sheet flows contributing to the topography. Seismic reflection and refraction experiments [*Harding et al.*, 1991; *Christeson et al.*, 1992] show that lava flows, which create seismic layer 2A, must routinely extend at least a kilometer or two from the axis at fast and very fast spreading rates. Backscatter data from within the EW9105 survey area [*Macdonald et al*, 1989] suggests that individual flows may extend up to 18 km off axis and be up to 70 m thick. It is likely that such flows are episodic, producing variations in the thickness of layer 2A and by consequence variations in surface topography.

The speculation that accumulating lava flows is a significant contributing factor to the formation of abyssal hills appears to be at odds with deep-tow observations [*Lonsdale*, 1977; *Bicknell et al.*, 1987] that maintain faulting is the primary source of topographic variation for EPR abyssal hill morphology. It also does not appear to be consistent with our own conclusion that faulting is the primary variable in abyssal hill segmentation. A possible way to reconcile these different views is to postulate that the component of morphology associated solely with accumulating flows undulates on distance scales (perpendicular to the axis) larger than the characteristic width of fault-created morphology. It is unlikely that deep-tow observations could identify such long-wavelength undulations, especially if the height variation is of the order of or less than the rms height of fault-generated topography. The observed variations in characteristic width may be explained by variations in the intensity of undulations in volcanic construction, which might be quite random along southern EPR segments but more systematic along northern EPR segments.

Unfortunately, it is very difficult to envision how variations in rms heights can be controlled by the faulting process, while at the same time variations in characteristic width are controlled by the volcanic process. For now we can only suggest that each parameter is somehow sensitive to different influences on the morphology. It is of course possible that the apparent relationship between shallow magma supply and characteristic width along both northern and southern EPR segments is either noncausal or a coincidence and that the characteristic width is fault controlled. Recent theoretical work by A. Malinverno and P. Cowie (submitted manuscript, 1992) provides a possible basis for this alternative hypothesis. Their work suggests that the characteristic width of faulted morphology is controlled by (i.e., positively correlated with) the strength of the faulted lithosphere, parameterized by elastic thickness. Thus, while the amount of strain, and by consequence the rms height may vary systematically along axis, if the elastic thickness does not change, then neither will the characteristic width. A recent study of the EW9105 gravity data by *Wang and Cochran* [1993] does in fact show that the elastic thickness is relatively constant in this survey area, providing possible support for this hypothesis. On the other hand, it is likely that elastic thickness along northern EPR segments increases toward segment ends as the magma supply at all levels decreases. In this case the alternative hypothesis would predict an increase in characteristic width toward the segment ends, in direct contradiction of the observation [*Goff*, 1991].

Edge-Driven Microplate Dynamics

The dramatic increases in both rms height (Figure 4) and characteristic width (Figures 5 and 6) along the W1 corridor approaching the ridge adjacent to the 8°38'S OSC suggest a causative relationship between the two. *Goff et al.* [1993] identified this ridge is at least in part a compressional feature associated with a microplate-style rotation of a block just to the south of this ridge and bounded east and west by active rifting. If true, then the large and wide undulations, which run parallel to the abyssal hill fabric and lie to the north of the east-west ridge, may be a further consequence of this compression; perhaps a buckling of the lithosphere along an axis of preexisting weakness (the abyssal hill faults).

Lineament Curvature at the Ridge-Transform Intersection

The EPR axis begins to curve toward the Wilkes transform complex approximately 40 km north of the W3 fracture zone trace (Plate 1 and Figure 1). This "radius of curvature" is considerably larger than observed at most other EPR ridge-transform intersections (including the Quebrada, Discovery, Gofar and Yaquina transforms along the southern EPR (based on maps of *Lonsdale* [1989]) and the Clipperton and Siqueiros transforms along the northern EPR (based on maps of *Macdonald and Fox* [1988])), where the radius of axis curvature generally does not exceed 10 km. The closest analogy to the large radius of curvature at the northern Wilkes-EPR intersection occurs on the northward extension of the rise axis at the southern Orozco-EPR ridge transform intersection where another large overlapping spreading system (the Orozco "picoplate") occurs [*Madsen et al.*, 1986; *Macdonald et al.*, 1992]. We thus speculate, without elaboration on root causes, that the rotating Wilkes nannoplate is responsible for the rotation of the stress field which is causing the curvature of the ridge axis. Irrespective of the reason for its existence, however, it is likely that the stress field responsible for rotating the EPR axis is also responsible for the rotation of adjacent abyssal hills (Figure 7).

Significant differences exist between the curvature of the axis and the curvature of adjacent abyssal hill lineaments at the EPR-Wilkes ridge-transform intersection. In particular, the radius of curvature of abyssal hill lineaments is noticeably larger (Figure 7). We first note that this difference implies that the curvature in abyssal hill lineaments must be controlled by the normal faulting process occurring on the ridge flanks. The only alternative is that the curvature in lineaments are controlled by axial volcanic construction. If the latter were true, then we expect that any such feature created along the axis will maintain its plan view shape when rafted onto the flanks; that is, we will expect axis and abyssal hill curvature to be identical. We speculate that the discrepancy between axis and abyssal hill lineament curvature reflects a difference in the response of plastic deformation (which occurs in a narrow zone about the axis) and brittle deformation (which occurs primarily > 2 km from the axis) to a rotation of the stress field. Under this scenario, the orientation of faults is permanently skew to the orientation of the ridge in the vicinity of a rotation in the stress field.

CONCLUSIONS

Quantitative characterization of abyssal hill morphology within the EW9105 survey area has enabled us to make the following primary observations and hypotheses.

1. The rms height of abyssal hill morphology (Figure 4) is negatively correlated with the width of the 5- to 20-km-wide crestal high, consistent with the observations of *Goff* [1991] for northern EPR abyssal hill morphology. Combined with the observations of *Macdonald and Fox* [1988] regarding ridge segmentation along the northern EPR and those of *Cochran et al.* [1993] regarding ridge segmentation within the EW9105 survey area, these observations lead us to hypothesize that the strain associated with surface normal faulting is controlled by the upwelling/temperature structure and/or the size of partial melt zone beneath the ridge axis. Three possible mechanisms were discussed which might explain such a relationship: the thickness of the brittle layer as determined by the temperature structure, a mechanical decoupling between upper and lower lithosphere by the partial melt zone, and a thermal buffering against rapid cooling of the lithosphere by the partial melt zone.

2. The characteristic abyssal hill width (Figure 5) displays no systematic variation with segmentation within the EW9105 survey area. This observation contrasts with that of *Goff* [1991] for northern EPR abyssal hill morphology, in which characteristic widths tended to be smallest at segment ends and largest toward the

middle of segments. These contrasting observations lead us to speculate that the shallow magma supply (which likewise varies systematically along the individual segments on the northern EPR, while being nearly constant along individual segments on the southern EPR [*Cochran et al.*, 1993]) may be exerting some influence on this off-axis variable. To explain such a relationship we speculate that lava flows which extend several kilometers from the axis episodically build up significant contributions of longer-scale topographic relief. Alternatively, this relationship could be either noncausal or coincident, and faulting may control this parameter, possibly through the elastic thickness (A. Malinverno and P. Cowie, submitted manuscript, 1992).

3. As the ridge emanating from the 8°38'S OSC (Plate 1 and Figure 1) is approached from the north along the W1 corridor, the rms height and characteristic width (Figures 4, 5 and 6) increase to very large values compared to estimates from the adjacent E1 corridor. If as suggested by *Goff et al.* [1993] the Wilkes nannoplate region south of this ridge is undergoing edge-driven microplate-style rotation, then the increase in rms height and characteristic width may represent a buckling of the lithosphere along an axis of preexisting weakness (abyssal hill faults) in response to northward compressional stresses.

4. Within the 8°38'S-7°12'S segment, abyssal hill lineaments (Figure 7) are generally parallel to the ridge axis, mimicking variations in axis azimuth. Approaching the EPR-Wilkes ridge transform intersection, both the axis and abyssal hill lineaments rotate with a large "radius of curvature". These phenomena are probably related to the Wilkes nannoplate on the west flank. However, the rotation of abyssal hill lineaments occurs with a larger radius of curvature. This disparity implies an off-axis tectonic origin to abyssal hill lineament curvature (an axis constructional volcanic origin would create identical curvatures). This leads us to speculate that the difference between abyssal hill lineament and axis curvature reflect a difference in the response of brittle and plastic deformation mechanisms to a rotation of the stress field.

Acknowledgments. This research was supported by National Science Foundation grants OCE-9019741 (WHOI) and OCE-8911376 (Lamont). We are greatly indebted to Martin Kleinrock and Deborah Smith for helpful and stimulating discussion and to Bill Haxby for the software used to generate Figure 1. We also thank Margo Edwards, John Madsen and the associate editor Carol Raymond for helpful reviews. WHOI contribution 8220. Lamont-Doherty contribution number 5069.

REFERENCES

Bicknell, J. D., J.-C. Sempere, K. C. Macdonald, and P. J. Fox, Tectonics of a fast spreading center: A Deep-Tow and Sea Beam survey on the East Pacific Rise at 19° 30' S., *Mar. Geophys. Res.*, *9*, 25-45, 1987.

Burnett, M. S., D. W. Caress, and J. A. Orcutt, Tomographic image of the magma chamber at 12° 50' N on the East Pacific Rise, *Nature*, *339*, 206-208, 1989.

Chayes, D. N., D. W. Caress, W. B. F. Ryan, A. Malinverno, W. Menke, and C. Keeley, Status of Hydrosweep on the R/V Ewing: System operation and data processing, *Eos Trans. AGU*, *72* (44), Fall Meeting suppl., 488, 1991.

Chen, Y., and W. J. Morgan, Rift valley/no rift valley at mid-ocean ridges, *J. Geophys. Res.*, *95*, 17,571-17,581, 1990.

Choukroune, P., J. Francheteau, and R. Heikinian, Tectonics of the East Pacific Rise near 12° 50' N: A submersible study, *Earth Planet. Sci. Lett.*, *68*, 115-127, 1984.

Christeson, G. L., G. M. Purdy, and G. J. Fryer, Structure of young upper crust at the East Pacific Rise near 930'N, *Geophys. Res. Lett.*, *19*, 1045-1048, 1992.

Cochran, J. R., J. A. Goff, A. Malinverno, D. J. Fornari, C. Keeley, and X. Wang, Morphology of a "superfast" mid-ocean ridge crest and flanks: The East Pacific Rise, 7°-9°S, *Mar. Geophys. Res.*, *15*, 65-75, 1993.

CYAMEX, First manned submersible dives on the East Pacific Rise at 21°N (project RITA): General results, *Mar. Geophys. Res.*, *4*, 345-379, 1981.

Detrick, R. S., P. Buhl, E. Vera, J. Mutter, J. Orcutt, J. Madsen, and T. Brocher, Multi-channel seismic imaging of a crustal magma chamber along the East Pacific Rise, *Nature*, *326*, 35-41, 1987.

Edwards, M. H., D. J. Fornari, A. Malinverno, and W. B. F. Ryan, The regional tectonic fabric of the East Pacific Rise from 12°50'N to 15°10'N, *J. Geophys. Res.*, *96*, 7995-8017, 1991.

Forsyth, D. W., Finite extension and low-angle normal faulting, *Geology*, *20*, 27-30, 1992.

Goff, J. A., A global and regional stochastic analysis of near-ridge abyssal hill morphology, *J. Geophys. Res.*, *96*, 21,713-21,737, 1991.

Goff, J. A., Quantitative characterization of abyssal hill morphology along flow lines in the Atlantic Ocean, *J. Geophys. Res.*, *97*, 9183-9202, 1992.

Goff, J. A., and T. H. Jordan, Stochastic modeling of seafloor morphology: Inversion of Sea Beam data for second-order statistics, *J. Geophys. Res.*, *93*, 13,589-13,608, 1988.

Goff, J. A., and T. H. Jordan, Stochastic modeling of seafloor morphology: A parameterized, Gaussian model, *Geophys. Res. Lett.*, *16*, 45-48, 1989*a*.

Goff, J. A., and T. H. Jordan, Stochastic modeling of seafloor morphology: Resolution of topographic parameters by Sea Beam data, *IEEE J. Ocean Eng.*, *14*, 326-337, 1989*b*.

Goff, J. A., D. J. Fornari, J. R. Cochran, C. Keeley, A. Malinverno, The Wilkes transform system and "nannoplate", *Geology*, in press, 1993.

Harding, A. J., G. M. Kent, M. E. Kappus, and J. A. Orcutt, Examination of layer 2A between 850'N and 950'N on the East Pacific Rise using CDP data (abstract), *Eos Trans. AGU*, *72* (44), Fall Meeting suppl., 494, 1991.

Harrison, C. G. A., and L. Stieltjes, Faulting within the median valley, *Tectonophysics*, *38*, 137-144, 1977.

Kong, L. S. L., R. S. Detrick, P. J. Fox, L. A. Mayer, and W. B. F. Ryan, The morphology and tectonics of the MARK area from Sea Beam and Sea MARC I observations (Mid-Atlantic Ridge 23N), *Mar. Geophys. Res.*, *10*, 59-90, 1988.

Lewis, B. T. R., Periodicities in volcanism and longitudinal magma flow on the East Pacific Rise at 23°N, *Geophys. Res. Lett.*, *6*, 753-756, 1979.

Lin, J., and E. M. Parmentier, Mechanisms of lithospheric extension at mid-ocean ridges, *Geophys. J.*, *96*, 1-22, 1989.

Lister, C. R. B., Qualitative models of spreading-center processes, including hydrothermal penetration, *Tectonophysics*, *37*, 203-218, 1977.

Lonsdale, P., Structural geomorphology of a fast-spreading rise crest: The East Pacific Rise near 325'S, *Mar. Geophys. Res.*, *3*, 251-293, 1977.

Lonsdale, P., Segmentation of the Pacific-Nazca spreading center, 1°N-20°S, *J. Geophys. Res.*, *94*, 12,197-12,225, 1989.

Macdonald, K. C., and P. J. Fox, The axial summit graben and cross-sectional shape of the East Pacific Rise as indicators of axial magma chambers and recent volcanic eruptions, *Earth Planet. Sci. Lett.*, *88*, 119-131, 1988.

Macdonald, K. C., and B. P. Luyendyk, Investigation of faulting and abyssal hill formation on the flanks of the East Pacific Rise (21°N) using Alvin, *Mar. Geophys. Res.*, *7*, 515-535, 1985.

Macdonald, K. C., P. J. Fox, L. J. Perram, M. F. Eisen, R. M. Haymon, S. P. Miller, S. M. Carbotte, M.-H. Cormier, and A. N. Shor, A new view of the mid-ocean ridge from the behaviour of ridge-axis discontinuities, *Nature*, *335*, 217-225, 1988.

Macdonald, K. C., R. M. Haymon, and A. Shor, A 220 km^2 recently erupted lava field on the East Pacific Rise near lat 8°S, *Geology*, *17*, 212-216, 1989.

Macdonald, K. C., P. J. Fox, S. Miller, S. Carbotte, M. H. Edwards, M. Eisen, D. J. Fornari, L Perram, R. Pockalny, D. Scheirer, S. Tighe, C. Weiland, and D. Wilson, The East Pacific Rise and its flanks 8-18°N: History of segmentation, propagation and spreading direction based on SeaMARC II and Sea Beam studies, *Mar. Geophys. Res.*, *14*, 299-344, 1992.

Madsen, J. A., D. W. Forsyth, and R. S. Detrick, A new isostatic model for the East Pacific Rise crest, *J. Geophys. Res.*, *89*, 9997-10,015, 1984.

Madsen, J. A., P. J. Fox, and K. C. Macdonald, Morphotectonic fabric of the Orozco Transform fault: Results fro a Sea Beam investigation, *J. Geophys. Res.*, *91*, 3439-3454, 1986.

Madsen, J. A., R. S. Detrick, J. C. Mutter, P. Buhl, and J. C. Orcutt, A two- and three-dimensional analysis of gravity anomalies associated with the East Pacific Rise at 9°N and 13°N, *J. Geophys. Res.*, *95*, 4967-4987, 1990.

Phipps-Morgan, J., E. M. Parmentier, and J. Lin., Mechanisms for the origin of mid-oceanic ridge axial topography: Implications for the thermal and mechanical structure of accreting plate boundaries, *J. Geophys. Res.*, *92*, 12,823-12,836, 1987.

Renard, V., R. Heikinian, J. Francheteau, R. D. Ballard, and H. Backer, Submersible observations at the axis of the ultra-fast-spreading East Pacific Rise (17°30' to 21°30' S), *Earth Planet. Sci. Lett.*, *75*, 339-353, 1985.

Schouten, H., K. D. Klitgord, and D. G. Gallo, Edge-driven microplate kinematics, *J. Geophys. Res.*, *98*, 6689-6701, 1993.

Searle, R., GLORIA survey of the East Pacific Rise near 3.5°S: Tectonic and volcanic characteristics of a fast spreading mid-ocean rise, *Tectonophysics*, *101*, 319-344, 1984.

Sinton, J. M., and R. S. Detrick, Mid-ocean ridge magma chambers, *J. Geophys. Res.*, *97*, 197-216, 1992.

Smith, D. K., and J. Cann, Hundreds of small volcanoes on the median valley floor of the Mid-Atlantic Ridge at 24°-30°N, *Nature*, *348*, 152-155, 1990.

Tapponnier, P., and J. Francheteau, Necking of the lithosphere and mechanics of slowly accreting plate boundaries, *J. Geophys. Res.*, *83*, 3955-3970, 1978.

Toomey, D. R., G. M. Purdy, S. C. Solomon, and W. S. D. Wilcock, The three-dimensional seismic velocity structure of the East Pacific Rise near latitude 9°30'S, *Nature*, *347*, 639-645, 1990.

Wang, X., and J. R. Cochran, Gravity anomalies, isostasy, and mantle flow at the East Pacific Rise crest, *J. Geophys. Res.*, in press, 1993.

J. R. Cochran, D. J. Fornari, and A. Malinverno, Lamont-Doherty Earth Observatory, Palisades, NY 10964.

J. A. Goff, University of Texas Institute for Geophysics, 8701 N. MoPac Expressway, Austin, TX 78759-8345.

(Received October 23, 1992;
revised April 5, 1993;
accepted April 22, 1993.)